Double-Helical Ultrastructure of Polycationic Dendronized Polymers Determined by Single-Particle Cryo-TEM

Christoph Böttcher,*[a] Boris Schade,[a] Christof Ecker,[b] Jürgen P. Rabe,*[b] Lijin Shu,[c] and A. Dieter Schlüter[c]

Abstract: The ultrastructure of cationic dendronized polymers (denpols) of third and fourth generations (**PG3** and **PG4**) in water was determined by using single-particle cryo-transmission electron microscopy (cryo-TEM). At concentrations in the region of 50 mg L^{-1}, networks of double-stranded fibers were revealed that exhibit well-defined diameters of 5.9 nm ± 0.4 nm for **PG3** and 7.4 nm ± 0.4 nm for **PG4**. The structure varies with progression along the fibers, and includes a double helix with a pitch of 7.0 ± 0.4 nm for **PG3** and 9.0 ± 0.4 nm for **PG4**. The formation of the double strands is attributed to the hydrophobic effect and limited crowding in the dendron shell of the third and fourth generation denpols investigated. From solutions of lower concentrations (around 10 mg L^{-1}), isolated molecular fibers were adsorbed onto high-energy surfaces and examined by performing scanning force microscopy (SFM) on mica, and after staining, TEM on glow-discharged carbon films. In both cases, characteristic undulations of single strands were observed, which are attributed largely to the adsorption process.

Keywords: dendrimers · double helix · polyelectrolytes · self-assembly · supramolecular chemistry

Introduction

Dendronized polymers (denpols) consist of a backbone to which dendrons of various generations are attached in a tightly packed sequence.[1] Denpols with higher-generation dendrons (e.g., third or fourth generation) form large molecular objects with a near-cylindrical shape, which can have dimensions of 4–7 nm in diameter and 200–400 nm in length, as observed by small-angle neutron scattering experiments in organic solvents[2] and scanning force microscopy (SFM) using adsorption onto mica[3]. Dendrons carrying peripheral, protected amines have been used to perform surface modifications of denpols under various aspects.[4] Upon deprotection and quaternization of these amines, the entire structures were converted into a novel kind of polyelectrolyte, with up to 16 positive charges every 0.25 nm along the backbone. Well-defined complexes have been formed from double-stranded DNA (dsDNA), an oppositely charged natural polyelectrolyte, in which the DNA wraps around the denpol.[5] However, the resolution of SFM images produced in the tapping-mode is insufficient to image directly the ultrastructure of either the complex, or the denpol itself. This led us to investigate the native structure and conformation of two positively charged representatives in water by performing cryo-transmission electron microscopy (cryo-TEM). For comparison, the same denpols were investigated as dry adsorbates on high-energy surfaces by SFM, and, after staining, by TEM.

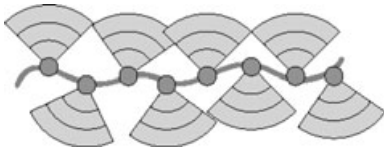

[a] Dr. C. Böttcher, Dr. B. Schade
Freie Universität Berlin
Forschungszentrum für Elektronenmikroskopie
Fabeckstrasse 36a, 14195 Berlin (Germany)
Fax: (+49) 30-838-56589
E-mail: bottcher@chemie.fu-berlin.de

[b] Dr. C. Ecker, Prof. Dr. J. P. Rabe
Humboldt University Berlin, Department of Physics
Newtonstrasse 15, 12489 Berlin (Germany)
Fax: (+49) 30-209-37632
E-mail: rabe@physik.hu-berlin.de

[c] Dr. L. Shu, Prof. Dr. A. D. Schlüter
Freie Universität Berlin, Institut für Chemie
Takustrasse 3, 14195 Berlin (Germany)
New address: Swiss Federal Institute of Technology (ETH)
Department of Materials, Institute of Polymers, HCI J541
8093 Zürich-Hönggerberg (Switzerland)

Cryo-TEM is currently the only technique that, in principle, allows direct access to information concerning the interior structure of large molecules and supramolecular assem-

 DOI: 10.1002/chem.200401145

blies in their native state.[6] Unfortunately, due to the low contrast of the images obtained, the inherent information in many cases cannot be extracted directly from the raw image data. However, by aligning and summating several projection images of individual motifs in the identical spatial orientation, the signal can be enhanced with respect to the random background noise. A set of such noise-reduced, composite images, the so-called "class averages", represents projections of an object's different spatial orientations, and can be used to reconstruct three-dimensional structures that include significant structural details. This "single-particle" approach is now an established method for the determination of three-dimensional structures of, for example, proteins.[7] It has recently been used to elucidate the three-dimensional organization of structurally well-defined dendrocalixarene micelles,[8] and by using a modified form of the approach, the three-dimensional organization of helical, fibrous aggregates formed by amphiphilic hexonamides has been determined.[9]

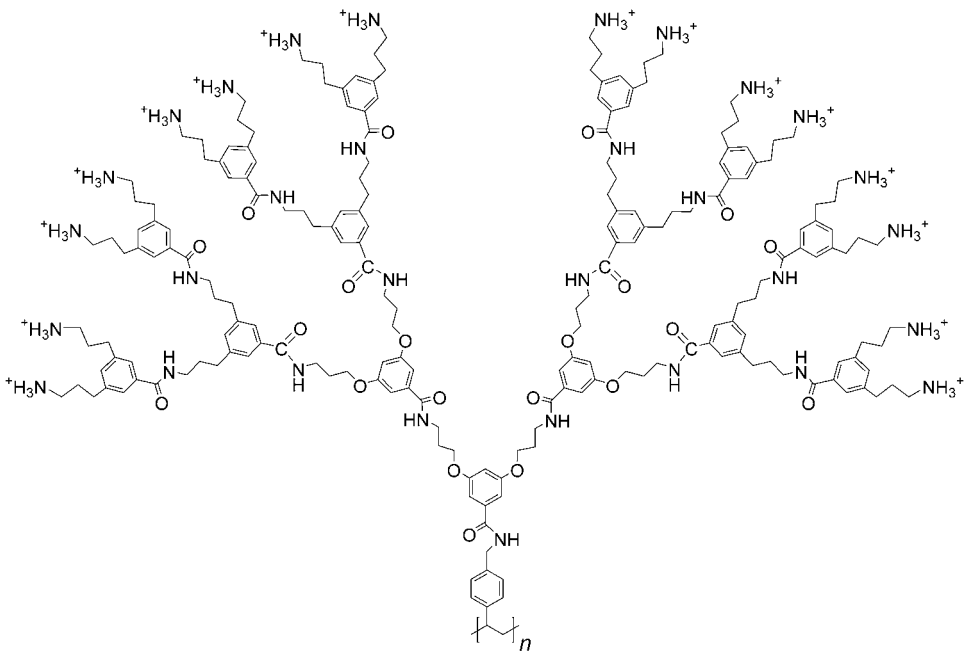

Figure 1. The chemical structure of **PG4** (counterion: $CF_3CO_2^-$).

Polymers adsorbed on high-energy surfaces, such as mica, can be imaged in their native states (i.e., without staining), by using scanning force microscopy. Alternatively, they can be prepared on glow-discharge-treated carbon support films, after staining by TEM. Image analysis of dry, dilute, submonolayers reveals information about the molecular conformations at the surfaces. Due to the substantial adsorption forces, the structures observed may be different from the structure in solution.[10]

Results and Discussion

Third and fourth generation denpols (**PG3** and **PG4**) with polystyrene backbones (Figure 1, structure **PG3** not shown), which have 8 and 16 positive charges per repeating unit, respectively, were synthesized by treating (deprotecting) their trimethylsilylethyleneoxycarbonyl- (Teoc) protected precursors with trifluoroacetic acid.[11] Due to the divergent mode of their synthesis, both polymers have approximately the same average degree of polymerization (number-average degree of polymerization (P_n) = 460 and weight-average degree of polymerization (P_w) = 830), corresponding to backbone lengths in the stretched conformation of 120 nm and 210 nm, respectively.[12] Their structural perfection was quantified to be greater than 97 %.[13] Because the polyelectrolytes were yielded following deprotection of the corresponding denpols that contained protected amines, by using trifluoroacetic acid, the ammonium ions' counterions were trifluoroacetate ions. The degree of deprotection was quantified by using high-field NMR spectroscopy to be greater than 98 %.[14] Both polymers were independently prepared in their native solvent (water) by vitrification in liquid ethane at its freezing point ("ultraquickfreezing"), and were directly visualized in a transmission electron microscope. Preparation and microscopy techniques followed well-established methods.[15]

Figure 2 shows a representative cryo-TEM micrograph of **PG4** presenting the cationic denpols as a network of fibers.

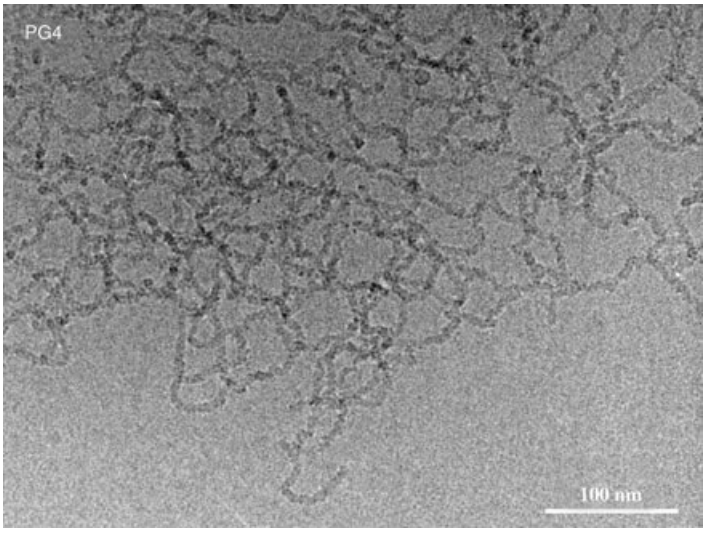

Figure 2. Representative cryo-TEM image of the **PG4** fiber network embedded in a vitrified layer of water.

PG3 revealed a similar overall appearance (not shown). Individual fiber motifs can be clearly discerned; however, faint variations in density suggested the need to apply further image processing and classification procedures. For this, 918 individual motifs of **PG3**, and 1181 of **PG4** were interactively extracted as 100×100 pixel fields (17.1×17.1 nm on the microscopical scale) from digitized micrographs. After filtering to suppress high-frequency background noise, established nonbiased "reference-free" alignment and automatic classification procedures were performed, which included multivariate statistical analysis and automated hierarchical classification schemes.[16] Individual images corresponding to identical spatial object orientations (=identical Euler angles) could thus be identified, extracted, aligned, and summed to yield class sum images with an enhanced signal-to-noise ratio.

Galleries of class averages for **PG3** and **PG4** are given in Figure 3a and b, respectively. Despite obvious differences in the ultrastructural[17] patterns, which are discussed below, the diameters of the motifs obtained for both denpol generations appear significantly monodisperse and amount to $5.9\,\text{nm}\pm0.4$ nm for **PG3** and $7.4\,\text{nm}\pm0.4$ nm for **PG4**. The most striking feature observed for almost all given classes is that of low density (i.e., dark) areas in the central parts of the fibers, which in some cases even possess a pronounced, braid-like structure (prominent in, for example, location 6 (**PG3**) in Figure 3a, or locations 5 and 8 (**PG4**) in Figure 3b). This clearly suggests that segments of the fibers form structurally well-defined patterns. However, the three-dimensional organization to which the observed projection patterns are related remains to be shown.

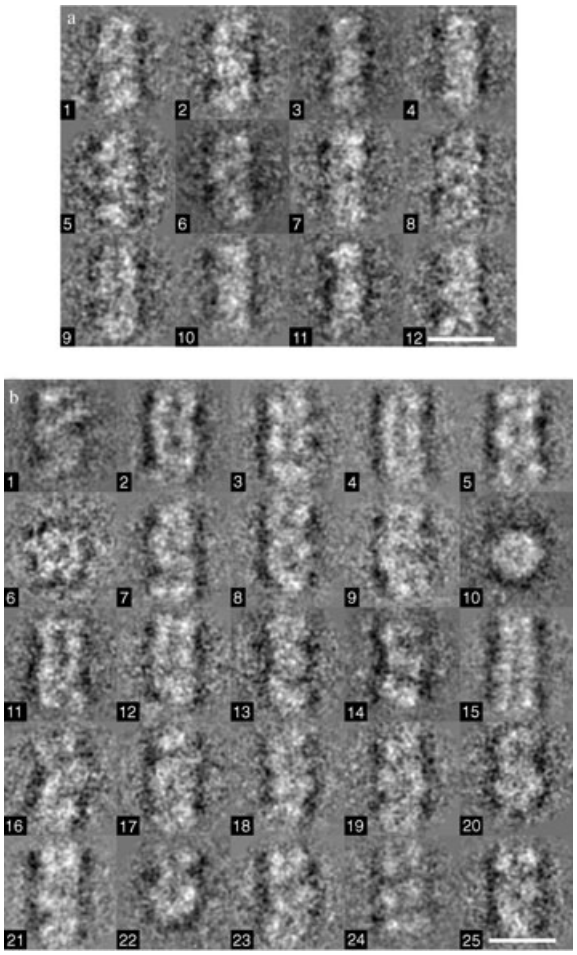

Figure 3. Class sum images obtained from several hundred individual fiber motifs of **PG3** (a) and **PG4** (b) (see text for details). Scale bar represents 10 nm.

One of the authors has reported reconstruction of the three-dimensional structure of helical, fibrous aggregates, which are spontaneously formed by amphiphilic hexonamides in aqueous solution.[9] In this case, the fundamental idea of reconstruction was based on the fact that one single projection of a perfect helix is sufficient to retrieve complete 360° tomographic information. However, the denpol motifs reported in this present study were somewhat different, in that the observation of different class images definitely suggests structural variations in their three-dimensional organization. Nevertheless, a number of very regular and symmetrical repetitive fiber segments (e.g., location 5 in Figure 3b) can be seen and allow, at least in this particular case, for the three-dimensional reconstruction by using the approach cited above. Once the calculation has provided insights into the principal three-dimensional, spatial organization of the fiber, it is expected that the less symmetrical class sum images observed can be interpreted.

From the projection pattern of a helix, the full periodic repeat (pitch) can be retrieved from the maxima determined in the autocorrelation function of the image.[9] As the pattern of location 5 (Figure 3b) appears to be almost perfectly mm symmetrical (mm=two mirror axis perpendicular to each other), C_2-symmetrization was applied to the sum image (Figure 4a) to remove minor symmetry deviations. By vertical displacement of the motif obtained in 360 steps (i.e., cyclical shift in 1° steps) over the full helical pitch, a set of projections over the full tomographic range (360°) was obtained. This set of images contains the full three-dimensional volume information and can be used as input for the "exact filter" reconstruction algorithm. Figure 4b shows the surface-rendered view of the data, and indicates that the

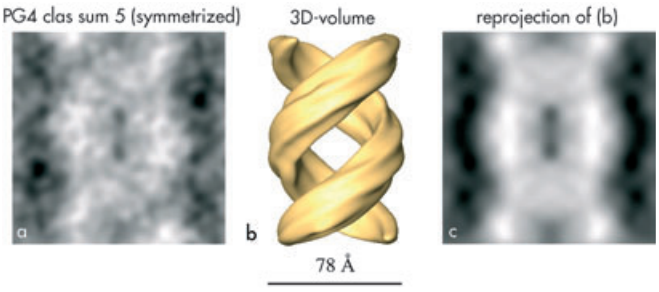

Figure 4. a) The C_2-symmetrized, two-dimensional class sum image of location 5 taken from Figure 3b. b) Calculation of the three-dimensional volume obtained from (a). c) The reprojection of (b) into the three-dimensional volume. This appears to be very similar to the input data (a) and proves the consistency of the reconstruction. Note that the threshold of the three-dimensional volume is deliberately chosen so that the three-dimensional organization of the strands can be clearly distinguished.

three-dimensional volume consists of two centrosymmetrically and helically wound fiber strands. A reprojection into the reconstructed volume, the consistency of which depends on the numerical deviation from the input data, satisfactorily reproduces the data input (Figure 4c).

The results reveal two surprising facts. Firstly, as is already obvious from the raw image data, the constituent molecules, which range from 100 to 200 nm in length, must have undergone a substantial end-on aggregation process. This is because we find exclusively networks of fibers on the micrometer scale. Secondly, class sum images suggest distinct packing motifs within the aggregates, for which the density profile, in combination with the reconstructed three-dimensional volume, indicate that two separated strands are involved in the structural conformation. The reconstruction even points to a helical arrangement of the constituents in some of the fiber segments. However, the existence of structurally different class averages suggests that variations in the supramolecular arrangement are also present. This could be explained by the regular arrangement being affected by entanglements or strand displacement. If the strands are vertically or horizontally displaced with respect to each other, characteristic density changes in the projection images occur. Location 16 in Figure 3b, as an example, shows irregular, low-density areas and a deformed outer contour. Similar effects can be seen for locations 1, 9, or 11. In location 15 in Figure 3b, the strands are presumably organized in a completely parallel arrangement and, therefore, do not display crossings, in opposition to almost all other classes. Of special interest are the unusually structured locations, such as 20 or 22 (Figure 3b). To our understanding, these classes represent typical fiber end-caps. Location 22 is a typical side-view of an end-cap and clearly shows that its constituent fibers do not terminate abruptly, but rather form a loop-like turn with a slight broadening of the cap. On the other hand, locations 6 and 10 represent top-views of the fiber, which is oriented parallel to the incident electron beam. Here again, the continuous outer, high-density area formed by the circumferential arrangement of the constituent fibers encapsulates an artery-like, low-density area in the fiber center.

The important questions of what the structural arrangement on the molecular scale looks like, and what the driving force for this arrangement is, remain unanswered. We suggest that single strands in solution are energetically unfavorable, as circumferential shielding of the hydrophobic backbones of the molecules from the polar solvent cannot be effectively accomplished by the number of hydrophilic branches. Even on the fourth generation level, the dendrons may not provide a shell that is dense enough to protect the interior of the denpols against water. This is supported by the successful attempt to force all dendrons in a model of the denpol into a half cylinder. Figure 5 displays a van der Waals representation of a half cylinder exhibiting the hydrophobic backbone to the flat side, and the hydrophilic and finally charged branches to the curved side, facing the surrounding water. This structure has not been rigorously energy-minimized, but was used to estimate the diameter of a double-stranded fiber to be around 8 nm for **PG4**, which is in reasonable agreement with the value obtained from the reconstruction of class sum 5 (7.4 nm) in Figure 3b. However, the weak distance-dependence and the nondirectionality of the electrostatic interactions permit relatively high flexibilities, which explains the observation of several structural alterations. The latter effect may also be a consequence of stresses during preparation that introduce different kinds of bends, shifts, and unwinding effects to the aggregates. Nevertheless, the tight and regular double-helical organization may be the most favorable arrangement and would represent a double helix produced from two polymers that has, to the best of our knowledge, by far the largest diameter. Much smaller double helices in solution are stabilized by hydrogen bonds, aromatic–aromatic interactions, and metal coordination.[18] In a single crystalline phase, the sum of other noncovalent interactions may lead to a double helix (isotactic poly(methyl methacrylate)).[19] In contrast, there is very little evidence for double helices of polymers in solution. Recently, one case has been suggested, mainly on the basis of SFM tapping-mode images and the interpretation of the apparent width of single adsorbates. However, this did not take into account the broadening due to a finite tip radius.[20] Furthermore, rod-like polyelectrolytes have been found to associate anisotropically into cylindrical micelles with a diameter of 3.4 nm, but a more detailed internal structure has not been reported.[21]

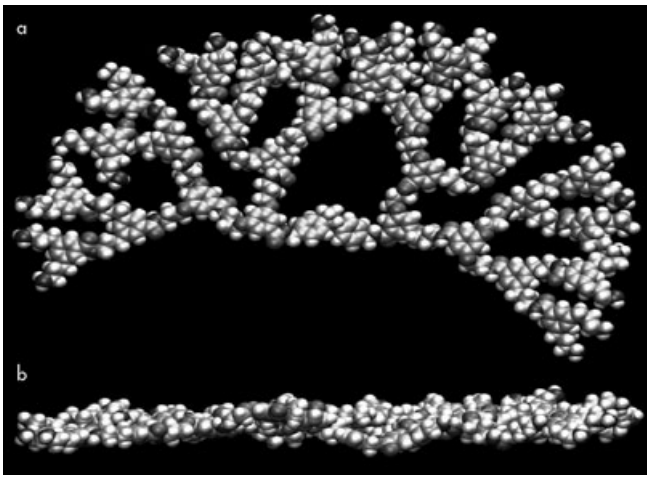

Figure 5. Side (a) and top (b) view of a van der Waals representation of two consecutive repeat units of **PG4**, indicating that there is enough space for two independent **PG4** chains to form a dimeric aggregate that presents the positive charges to the outside and protects the apolar interior from the water. The longest cross-sectional length in this model is approximately 8 nm.

To compare results of the cryo-TEM experiments with those of SFM and, after staining, TEM at ambient temperatures, we deposited the denpols onto high-energy surfaces, that is, freshly cleaved mica for SFM imaging, and glow-discharge-treated carbon films for TEM. At relatively high concentrations, such as those used for the cryo-TEM experiments, we observed collapsed networks, which could not be

resolved on the molecular scale. At lower concentrations of around 10 mg L^{-1}, both SFM and TEM images (Figures 6 and 7, respectively) revealed no networks, but rather individual objects with lengths in the region of 100 nm, and with

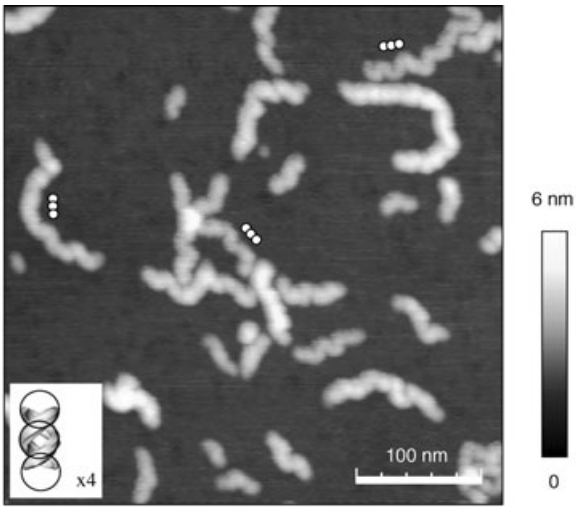

Figure 6. SFM tapping-mode image of **PG4** on mica. The white circles indicate the size of the proposed double helix.

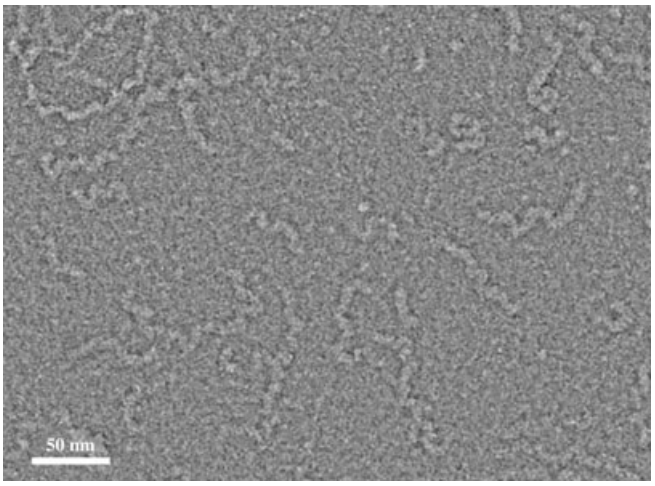

Figure 7. TEM image of **PG3**, which was deposited and dried on glow-discharged carbon film by using uranyl acetate (1% m/v) as contrasting material.

rather homogeneous heights and widths. The quantitative values for the latter could not, however, be readily interpreted, due to factors such as tip broadening, molecular compression, and tip adhesion in SFM, and staining artifacts in TEM. Therefore, we focussed on the two-dimensional contours of the objects.

Characteristic for both the SFM and TEM images were linear, two-dimensional objects displaying undulations in the plane with a period in the range of 10 to 15 nm. Although the undulations may resemble helical conformations, we do not attribute them to the double helices found in the cryo-TEM experiments, because they have a larger pitch than the proposed double helix, as indicated in Figure 6. Instead, due to the strong adhesion of the denpols to the mica, it is expected that the contour will reflect the adsorption process. Also, the stiffness of the chain and the three-dimensional coil structure will play a role. Although a rigorous distinction between the different contributions goes beyond the scope of this paper, we can conclude that the denpol fibers interact strongly with the substrate, thereby causing a meandering backbone structure on the surface, which neither exists in solution, nor is an equilibrated structure in two dimensions. Similar undulations were observed for other macromolecules, such as **PG1**, **PG2**, and DNA,[22] as well as brushes with poly(methyl methacrylate) side chains, though the latter was attributed to the asymmetric attachment of the side-chains to the polymer backbone.[23]

Conclusion

We have determined the ultrastructure of polycationic dendronized polymers in aqueous solutions of relatively high concentrations to be a network of double-stranded denpols. The dimer formation of the denpols is attributed to the hydrophobicity of the polystyrene backbone, and the polydispersity leads to both the folding of denpols back on themselves, and network formation due to braiding of different chains. The latter is reminiscent of the braiding seen with dsDNA,[24] and provides opportunities for the further investigation of nanoconstructions by using, for example, denpols of various flexibilities and charge densities, as well as those of opposite charges.

Experimental Section

Cryo-TEM: Droplets (total volume 5 μL) of aqueous, buffered (HEPES, pH 7.5) solutions of polymers at a concentration of 45 ng μL^{-1} were applied to perforated carbon-covered 200 mesh grids (R1/4 batch of Quantifoil Micro Tools, Jena, Germany), and were hydrophilized by plasma treatment (60 s at 8 W in a BALTEC MED 020 device, BALTEC, Liechtenstein). The supernatant fluid was removed by using filter paper until an ultrathin layer of the sample solution remained, which spanned the holes of the carbon film. The samples were immediately vitrified by propelling the grids into liquid ethane at its freezing point (90 K) operating a guillotine-like plunging device under humidity- and temperature-controlled conditions.[25] The vitrified samples were subsequently transferred under liquid nitrogen into a Philips CM12 transmission electron microscope (FEI Company, Oregon, USA) equipped with the Gatan (Gatan, California, USA) cryoholder and stage (Model 626). Microscopy was carried out at a sample temperature of 94 K by using the low-dose protocol of the microscope at a primary magnification of 58 300× and an accelerating voltage of 100 kV (LaB_6 illumination). In all cases the defocus was set to 1.2 μm, which corresponds to a first zero of the phase-contrast transfer function at 2.1 nm.

Optically sound micrographs (the absence of astigmatism or drift was checked by conducting laser optical diffraction) were digitized at a resolution of 2400 dpi by using a "Primescan" Heidelberg drum scanner (Heidelberger Druckmaschinen, Heidelberg, Germany). A pixel resolution of 1.71 Å was obtained at the primary electron optical magnification of 58 300×, used for imaging.

A total of 913 individual motifs of **PG3** and 1181 motifs of **PG4** were interactively extracted as 100×100 pixel fields and used in further image processing procedures, with the aid of IMAGIC5 software (Image Science, Berlin, Germany).

Negative staining: An amount (5 μL) of an aqueous buffered solution (HEPES, pH 7.5) of **PG3** at a concentration of 25 ng μL^{-1} was placed on hydrophilized (see above) carbon-coated copper grids, and supernatant fluid was removed by using filter paper. A droplet of uranyl acetate (1% w/v) was added for 60 s, subsequently removed, and the sample was allowed to air-dry.

Scanning force microscopy: The molecules were deposited by spin coating them (at 50 rps) from dilute aqueous solutions onto freshly cleaved mica surfaces. The surface density of the adsorbed molecules was adjusted by varying the concentration of the solution from 1 to 10 mg L^{-1}. SFM was carried out at room temperature in air, using a commercial instrument (Nanoscope IIIa, Digital Instruments), and silicon cantilevers (Olympus) with a resonance frequency of about 300 kHz and a force constant of 42 N m^{-1}. All measurements were taken in the tapping mode. Image backgrounds were removed by fitting to first-order polynoms. No further image enhancement was applied.

Acknowledgement

This work was supported by the Deutsche Forschungsgemeinschaft (Sfb 448 "Mesoscopically Organized Composites" TPs A1, A11, and C6), which is gratefully acknowledged.

[1] A. D. Schlüter, J. P. Rabe, *Angew. Chem.* **2000**, *112*, 860–880; *Angew. Chem. Int. Ed.* **2000**, *39*, 864–883; A. Zhang, L. Shu, Z. Bo, A. D. Schlüter, *Macromol. Chem. Phys.* **2003**, *204*, 328–339; A. D. Schlüter in *Top. Curr. Chem., Vol. 245: Functional Molecular Nanostructures* (Ed.: A. D. Schlüter), Springer, **2005**, pp. 151–191.

[2] S. Förster, I. Neubert, A. D. Schlüter, P. Lindner, *Macromolecules* **1999**, *32*, 4043–4049.

[3] C. Ecker, N. Severin, L. Shu, A. D. Schlüter, J. P. Rabe, *Macromolecules* **2004**, *37*, 2484–2489.

[4] For example, see: J. Barner, F. Mallwitz, L. Shu, A. D. Schlüter, J. P. Rabe, *Angew. Chem.* **2003**, *115*, 1967–1979; *Angew. Chem. Int. Ed.* **2003**, *42*, 1932–1935.

[5] I. Gössl, L. Shu, A. D. Schlüter, J. P. Rabe, *J. Am. Chem. Soc.* **2002**, *124*, 6860–6865.

[6] M. Adrian, J. Dubochet, J. Lepault, A. W. McDowall, *Nature* **1984**, *308*, 32–36.

[7] For example, see: K. Ludwig, B. Baljinnyam, A. Herrmann, C, Böttcher, *EMBO J.* **2003**, *22*, 3761–3771; K. Ludwig, H. Fan, J. Dobers, M. Berger, W. Reutter, C. Böttcher, *Biochem. Biophys. Res. Commun.* **2004**, *313*, 223–229.

[8] N. Kellermann, W. Bauer, A. Hirsch, B. Schade, K. Ludwig, C. Böttcher, *Angew. Chem.* **2004**, *116*, 3019–3022; *Angew. Chem. Int. Ed.* **2004**, *43*, 2959–2962.

[9] C. Boettcher, H. Stark, M. van Heel, *Ultramicroscopy* **1996**, *62*, 133–139.

[10] E. Kellenberger in *Cryotechniques in Biological Electron Microscopy* (Eds.: R. A. Steinbrecht, K. Zierold), Springer, **1987**, pp. 35–63.

[11] Ammonium salts of most primary amines have pK_a values of 9–10. At pH 7, most of the amines are thus protonated. It is reasonable to assume that most of the amines of the denpols investigated in this study behave as independent, primary amines and thus, are also protonated. The degree of protonation was not determined. The counterion in all cases was trifluoroacetate.

[12] The molar mass was determined by performing gel permeation chromatography (GPC) with a polystyrene standard. This probably underestimates the actual molar mass.

[13] L. Shu, I. Gössl, J. P. Rabe, A. D. Schlüter, *Macromol. Chem. Phys.* **2002**, *203*, 2540–2550.

[14] Even when the NMR spectra of deprotected samples with very high signal-to-noise ratios were amplified considerably, there was no indication that deprotection was incomplete.

[15] J. Dubochet, M. Adrian, J.-J. Chang, J.-C. Homo, J. Lepault, A. W. McDowall, P. Schultz, *Quart. Rev. Biophys.*, **1988**, *21*, 129–228.

[16] M. van Heel, G. Harauz, E. V. Orlova, R. Schmidt, M. Schatz, *J. Struct. Biol.* **1996**, *116*, 17–24.

[17] The term ultrastructure was coined by microscopists and describes the level of organize that is below the level of resolution of the light microscope. In practice, it is a shorthand term for structure observed by using the electron microscope.

[18] D. J. Hill, M. J. Mio, R. B. Prince, T. S. Hughes, J. S. Moore, *Chem. Rev.* **2001**, *101*, 3893–4011.

[19] H. Kusanagi, H. Tadokoro, Y. Chatani, *Macromolecules* **1976**, *9*, 531–532.

[20] H. Schlaad, T. Krasia, M. Antonietti, *J. Am. Chem. Soc.* **2004**, *126*, 11307–11310.

[21] M. Bockstaller, W. Köhler, G. Wegner, D. Vlassopoulos, G. Fytas, *Macromolecules* **2000**, *33*, 3951–3953; M. Bockstaller, W. Köhler, G. Wegner, D. Vlassopoulos, G. Fytas, *Macromolecules* **2001**, *34*, 6359–6364.

[22] C. Ecker, Dissertation, Humboldt University, Berlin, submitted.

[23] S. S. Sheiko, M. Möller, *Chem. Rev.* **2001**, *101*, 4099–4124.

[24] N. C. Seeman, *Chem. Biol.* **2003**, *10*, 1151–1159; N. C. Seeman, *Nature* **2003**, *421*, 427–431.

[25] J. R. Bellare, H. T. Davis, L. E. Scriven, Y. Talmon, *J. Electron Microsc. Tech.* **1988**, *10*, 87–111.

Received: November 14, 2004
Published online: February 28, 2005